Dynamical and statistical emission of light charged particles in ^{36}Ar + ^{58}Ni induced reactions between 32 and 95 AMeV

A. Huerstel, P. Buchet, D. Dore, J-L. Charvet, R. Dayras, J. Guy, R. Legrain, L. Nalpas, C. Volant, G. Auger, et al.

Institut de Physique Nucléaire de Lyon

Université Claude Bernard

IN2P3 - CNRS

LYCEN 2000/27
March 2000

Dynamical and statistical emission of light charged particles in $^{36}Ar + ^{58}Ni$ induced reactions between 32 and 95 AMeV

A. Hürstel, et al., INDRA Collaboration

XXXVIII[th] International Winter Meeting on Nuclear Physics – Bormio – January 17-21, 2000

43, Boulevard du 11 Novembre 1918 - 69622 VILLEURBANNE Cedex - France

Dynamical and statistical emission of light charged particles in $^{36}Ar+^{58}Ni$ induced reactions between 32 and 95 AMeV*.

A. Hürstel[1], Ph. Buchet[1], D. Doré[1], J.L. Charvet[1], R. Dayras[1], J. Guy[1], R. Legrain[1], L. Nalpas[1], C. Volant[1], G. Auger[2], Ch.O. Bacri[3], N. Bellaize[4], F. Bocage[2], B. Borderie[3], R. Bougault[4], B. Bouriquet[2], R. Brou[4], A. Chbihi[2], J. Colin[4], D. Cussol[4], A. Demeyer[5], D. Durand[4], J.D. Frankland[2], E. Galichet[3,6], E. Genouin-Duhamel[4], E. Gerlic[5], D. Guinet[5], S. Hudan[2], P. Lautesse[5], F. Lavaud[3], J.L. Laville[2], J.F. Lecolley[4], C. Leduc[5], T. Lefort[4], A.M. Maskay[5], N. Le Neindre[4], O. Lopez[4], M. Louvel[4], A.D. Nguyen[4], P. Pawlowski[3], E. Plagnol[3], M. Parlog[7], M.F. Rivet[3], E. Rosato[8], F. Saint-Laurent[2,a], J.C. Steckmeyer[4], G. Tabacaru[7], B. Tamain[4], L. Tassan-Got[3], O. Tirel[2], E. Vient[4], M. Vigilante[8] and J.P. Wieleczko[2].

INDRA collaboration

1) DAPNIA/SPhN, CEA/Saclay, 91191 Gif sur Yvette Cedex, France
2) GANIL, CEA et IN2P3-CNRS, B.P. 5027, 14076 Caen Cedex, France
3) IPN Orsay, IN2P3-CNRS, 91406 Orsay Cedex, France
4) LPC, IN2P3-CNRS et Université, 14050 Caen Cedex, France
5) IPN Lyon, IN2P3-CNRS et Université, 69622 Villeurbanne, Cedex, France
6) Conservatoire National des Arts et Métiers, F-75141 Paris, Cedex, France
7) Institute of Physics and Nuclear Engineering, IFA, P.O. Box MG6, Bucharest, Roumania
8) Dipartimento di Scienze, Univ. Di Napoli, 80125 Napoli, Italy

Abstract

The rapidity distributions as well as the transverse energies of protons and alpha particles produced in the reaction $^{36}Ar+^{58}Ni$ have been studied as a function of impact parameter and bombarding energies from 32 to 95 A.MeV. Besides evaporation from excited quasi-projectile and quasi-target remnants, these particles are also produced in the overlapping zone between projectile and target with transverse energies proportional to the beam energy and with intensities which increases almost linearly as the impact parameter decreases. Above 50 A.MeV bombarding energy, the apparent temperatures of the evaporating quasi-projectile and quasi-target remnants become independent of bombarding energy and increase only slightly from 3 MeV for peripheral collisions to 5 MeV for central ones. This suggests that above 50 A.MeV bombarding energy most of the energy is dissipated in the overlap region between projectile and target whereas the excitation energy imparted to the projectile and target remnants does not evolve any further.

1. Introduction

How the energy of relative motion is dissipated in heavy ion collisions in the intermediate energy domain (~20 to ~100 A.MeV) is a recurrent question which has not yet received a satisfactory answer. A correlated question is how the dissipated energy is distributed amongst the reaction products and which fraction of this energy is thermalized into hot nuclei. Experimentally, they are very difficult questions to answer. In this energy regime, the relative velocities of the various sources of emission are comparable to the velocities of evaporated products by the hot thermalized nuclei. All relevant time scales (collision time,

* Experiment performed at GANIL.
a) Permanent address: DRFC/STEP CEA Cadarache, F-13108 Saint-Paul-lez-Durance, France.

relaxation time, life-time of the hot reaction products, etc) become comparable and the distinction between non-equilibrium and equilibrium emission is not obvious.

In the past, two basic scenarios were invoked to interpret the experimental data on projectile fragmentation in the intermediate regime [1-4]. Extrapolating up from the low energy regime, the mass (or charge) distributions of projectile-like fragments could be explained as resulting from a two-step process. In a binary encounter, the projectile and the target are excited to an amount which is governed by the impact parameter. The excited projectile and target evacuate their excitation energies by evaporating particles to yield the observed residues, the size of which is governed by the initial excitation energy. Extrapolating down from relativistic energy, the same data could be interpreted in the framework of the abrasion ablation model [5]. In this case, projectile (and target) fragments are considered as the remnants of a fast removal of the nucleons in the region of overlap between projectile and target. In previous measurements of the kinetic energy and of the charge (and/or the mass) distributions of the projectile-like fragments, it was not possible to solve this ambiguity [6, 7]. However, there were some hints that a purely binary scenario was too crude to describe properly the underlying mechanisms. In particular, it was not possible to reproduce the light particle spectra and angular distributions by just assuming two emission sources (the projectile and the target-like primary fragments) [8-12]. In effect there was an excess of energetic light particles around mid-rapidity which could not be explained by inelastic binary collisions.

With the advent of 4π array such as INDRA [13], it has become possible to get an overview of the collisions event by event. Although it is now clear [14] that the bulk of the reaction cross-section ends up, in the exit channel, with two primary excited fragments (projectile and target-like) which subsequently decay, a significant amount of mass has been evacuated before their formation and thus, the reactions cannot strictly be dubbed binary in the sense of deep inelastic collisions at low energy. In effect, besides standard evaporation from excited projectile and target-like fragments which have velocities close to the initial projectile and target velocities, a number of particles and light fragments are produced with intermediate parallel velocities [15-18]. The quantity of matter emitted in this mid-rapidity domain increases with decreasing impact parameter (at least down to mid-central collisions) [15, 16, 19]. Those particles and fragments are certainly produced in the early stage of the collisions and several mechanisms are invoked to explain their presence. Whereas nucleons and light clusters may be produced in primary nucleon-nucleon or nucleon-cluster collisions [20-23] in the region of overlap between projectile and target, heavier fragments may be produced at separation time by neck rupture or aligned fission [17,18] by dynamically deformed projectile and target like fragments.

In a recent study of the reaction $^{36}Ar+^{58}Ni$ from 52 to 95 A.MeV, it was shown [19] that light charged particles and also fragments were produced around mid-rapidity in excess of what would be expected from evaporation from excited quasi-projectiles and targets. Furthermore, the quantity of these products increases with decreasing impact parameters. Their transverse kinetic energy scales with the beam energy. Here we want to examine the consequences of this mid-rapidity emission on the excitation energies which are imparted to the primary projectile-like and target-like fragments. To do this and to limit the hypothesis on the underlying mechanisms, an attempt is made to unfold the proton and α-particle rapidity spectra. It is assumed that, in their own reference frame, the fully equilibrated primary projectile and target-like fragments evaporate light particles isotropically. Appropriate sources are introduced to describe the particles emitted between these two sources and they are characterized by their transverse energy.

2. Experimental method and event selection.

An ^{36}Ar beam provided by the GANIL facility was used to bombard 193 μg/cm^2 thick, self-supporting ^{58}Ni target at 32, 40, 52, 63, 74, 84 and 95 A.MeV. The beam intensity ~3-4×10^7 pps was such as to keep the probability of multiple interactions below 10^{-4}. The reaction charged products were detected with the 4π array INDRA [13] using a minimum biased trigger based on the multiplicity (M_c≥3 for 32A.MeV≤E_{lab}≤74A.MeV and M_c≥4 at 84 and 95 A.MeV). As the backward (92^0 to 176^0) ionization chamber of INDRA was not yet installed for this experiment, all fragments were identified by their atomic number only in the forward hemisphere. However, hydrogen an helium isotopes were fully identified from 3^0 to 176^0 (rings 2 to 17 of INDRA). In ring 1 (2^0 to 3^0) made of phoswiches this separation was not possible.

For the forthcoming analysis, we retain only events for which at least 50% of the incident linear momentum has been detected and for which the total charge multiplicity is greater than the trigger multiplicity. The effect of this selection [24] is to reject the most peripheral collisions in which the projectile fragment escaped through the hole between 0^0 and 2^0 whereas the target fragment had an energy below the detection thresholds. This selection enables us to explore essentially all the impact parameter range from peripheral to central collisions.

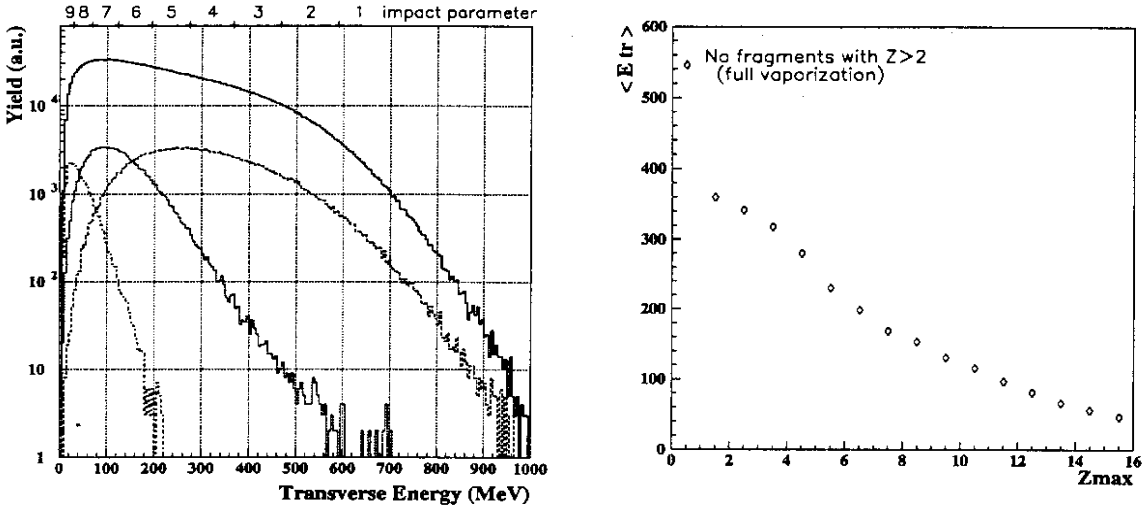

Fig. 1. *Left panel*). Yield as function of the total transverse energy for all selected events (black curve). The corresponding impact parameter scale is indicated on the top of the figure. The total transverse energy spectra for three selections in Z_{max}=16, 10 and 4 are given respectively by the dash- dotted, dotted and dashed curves. These spectra broaden and their most probable value increases as Z_{max} decreases. *Right panel*). Average total transverse energy $<E_{tr}>$ as a function of the atomic number Z_{max} of the biggest PLF fragment.

As we want to study the rapidity distributions as well as the average transverse energy of light charged particles as a function of the violence of the collisions we have to find a variable correlated to it. Often observables like the total transverse energy or the transverse energy carried out by light charged particles are considered as good impact parameter indicators [15, 16, 18, 19, 24] in our energy domain. Assuming a monotonous correlation between these observables and the measured cross-section which is supposed to depend geometrically on the impact parameter, one can deduced an impact parameter scale [25] shown in fig. 1 (left

panel). However, as we are interested in the evolution of the kinematical properties of light charged particles such as their transverse energies with the impact parameter, transverse energies (total or carried by light charged particles) cannot be used as an impact parameter indicator without introducing strong correlation effects. Instead, we choose to use the atomic number Z_{max} of the biggest projectile-like fragment (PLF) with a rapidity Y_{QP} greater than one half the projectile rapidity Y_P to characterize the violence of the collision. Total transverse energy spectra for three different values (16, 10 and 4) of the atomic number Z_{max} of the biggest PLF's are shown on fig. 1 (left panel). These spectra broaden and the most probable energy shifts toward higher values with decreasing Z_{max}. On fig. 1 (right panel) is shown the evolution of the average total transverse energy as a function of Z_{max}. From this figure, it can be inferred that the size of the biggest PLF is correlated with the violence of the collision, Z_{max} decreasing monotonously with the impact parameter. In the following analysis, the value of Z_{max} will be used to classify the events according to the violence of the collisions.

In order to make comparisons easier, a software detection threshold independent of detection angle was applied for each particle type (2 MeV for protons, 4 MeV for α-particles).

In fig. 2, are presented bidimensional plots of the relativistic invariant cross-sections for protons and α-particles produced at 52 and 95 A.MeV bombarding energies as a function of

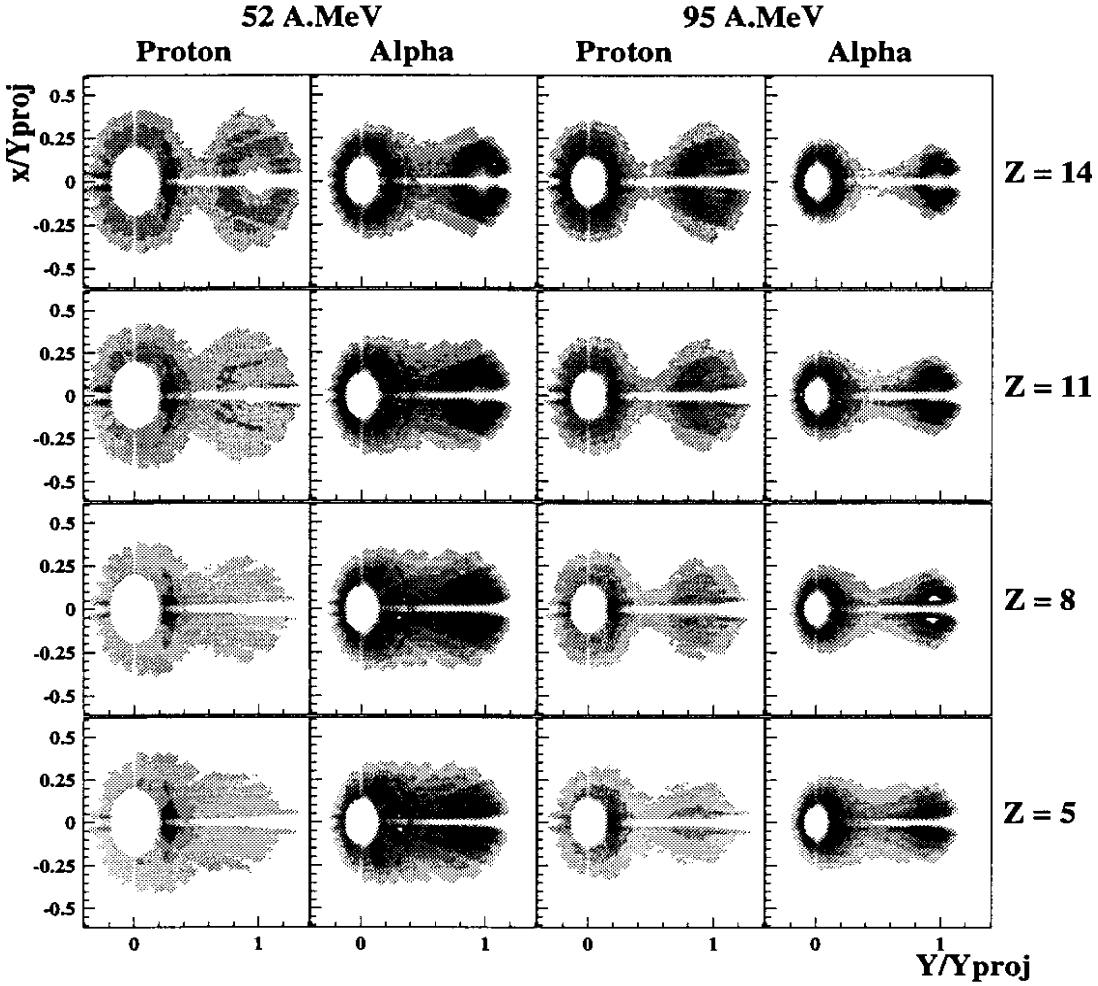

Fig. 2. Bidimensional plot, in the laboratory, of the relativistic invariant cross-sections for protons and α-particles at 52 and 95 A.MeV bombarding energies and for 4 values (14, 11, 8 and 5) of the PLF atomic number. To facilitate comparison between bombarding energy, both axes are normalized to the projectile rapidity Y_p.

the PLF atomic number Z_{max}. The holes centered around Y/Yp=0 result from the detection thresholds. For the most peripheral collisions ($Z_{max}\geq 11$) one clearly notices (particularly for α-particles) two separated sources of emission, centered respectively around the target and the projectile velocities. The separation between these two sources increases with bombarding energy but decreases as the impact parameter decreases (decreasing Z_{max}). However, one notices between these two sources, the presence of particles which cannot be explained by a simple overlap of the TLF and PLF emission spheres [19].

In fig. 3, are shown the experimental rapidity spectra (left panel, grey curves) for protons and their average transverse energies $\langle E_{tr}\rangle$ as a function of rapidity (right panel open diamonds) measured at 95 A.MeV for 4 different selections in Z_{max}. For peripheral collisions (large Z_{max}), the rapidity spectra are dominated by two well separated humps centered around the target and the projectile velocities. These humps broaden and overlap more an more strongly as the collisions become more violent (decreasing Z_{max}). The dips observed around Y/Yp=0 is due to the shadow of the target holder whereas the truncated shape of the target component has its origin in the detection thresholds. By contrast, the average transverse energy as a function of rapidity show a strong peak around mid-rapidity with a value ~20 MeV which is almost independent of the impact parameter. Near the projectile rapidity, Y/Y_p=1, the average transverse energy increases from ~5 MeV for Z_{max}=16 to about ~10 MeV for Z_{max}=4. Near the target velocity, the transverse energy is higher due to the detection thresholds. From the rapidity spectra alone, one may conclude that protons result essentially from evaporation by excited TLF's and PLF's. However the behavior of their average transverse energy as a function of rapidity clearly indicates that around mid-rapidity most of the protons have another origin as it has be shown in a previous work [19]. In the following, we will attempt to unfold the rapidity spectra in order to estimate their different components.

3. Unfolding procedure.

The primary TLF's and PLF's are considered as two main emission sources moving along the beam axis. Supposing that they have reach full equilibrium before to decay, we assume isotropic surface evaporation in the source reference frames with particle energy spectra given by:

$$\frac{d^3\sigma}{dE_{cm}d\Omega_{cm}} = \frac{N}{4\pi T}\frac{E_{cm}-B_c}{T}\exp(-\frac{E_{cm}-B_c}{T}) \quad ,$$

where T is the source temperature, E_{cm} the kinetic energy of the emitted particle in the source reference frame, B_c the Coulomb barrier and N a normalization coefficient. From this expression we can deduce the expected parallel velocity distribution in the laboratory:

$$\frac{d\sigma}{dv_{parlab}} = \frac{N}{2}\sqrt{\frac{m}{2T}}\exp(\frac{B_c}{T})\left[\frac{\sqrt{\pi}}{2}(1-\frac{2B_c}{T})[1-erf(x)]+x\exp(-x^2)\right] \quad ,$$

where m is the mass of the emitted particle, v_{parlab} its parallel velocity in the laboratory and v_s the velocity of the source. $x=\sqrt{\frac{B_c}{T}}$ for $|v_{parlab}|\leq\sqrt{\frac{2B_c}{m}}$ and $x=\sqrt{\frac{m}{2T}}|v_{parlab}-v_s|$ for $|v_{parlab}-v_s|\geq\sqrt{\frac{2B_c}{m}}$. We can also compute the transverse energy spectra versus v_{parlab}:

$$\frac{d^2\sigma}{dE_{per}dv_{parlab}} = \frac{N}{2T^2}\sqrt{\frac{m}{2}}\frac{E_{per}+\frac{1}{2}m(v_{parlab}-v_s)^2-B_c}{\sqrt{E_{per}+\frac{1}{2}m(v_{parlab}-v_s)^2}}\exp(-\frac{E_{per}+\frac{1}{2}m(v_{parlab}-v_s)^2-B_c}{T})$$

where E_{per} is the transverse energy of the emitted particle for a given parallel velocity v_{parlab}.

This last expression can be used to calculate the average transverse energy $<E_{tr}>$ of the particles as a function of the parallel velocity v_{parlab}. It can be shown that the values of $<E_{tr}>$ depend only slightly upon v_{parlab} and are essentially defined by the temperature T of the source and the Coulomb barrier B_c. Hence for $v_{parlab}=v_s$, one has $<E_{tr}>=3/2(T+B_c)$.
As mentioned previously, there is around mid-rapidity (MR) a production of particle which cannot be explained by primary PLF and TLF evaporation. We assume that these particles originate from the zone of overlap between the projectile an the target and that their production can be simulated by volume emission from a hot thermalized source emitting isotropically according to a maxwellian distribution:

$$\frac{d^3\sigma}{dE_{cm}d\Omega_{cm}} = \frac{N}{2(\pi T)^{3/2}}\sqrt{E_{cm}}\exp(-\frac{E_{cm}}{T}) \quad ,$$

where T is the source temperature, E_{cm} the kinetic energy of the emitted particle in the source frame and N a normalization constant. The particle parallel velocity distribution in the laboratory is given by:

$$\frac{d\sigma}{dv_{parlab}} = N\sqrt{\frac{m}{2\pi T}}\exp(-\frac{m(v_{parlab}-v_s)^2}{2T}) \quad ,$$

where m is the mass of the particle, v_{parlab} its parallel velocity in the laboratory and v_s the source velocity. The particle transverse energy spectra are described by the relation:

$$\frac{d^2\sigma}{dE_{per}dv_{parlab}} = \frac{N}{T}\sqrt{\frac{m}{2\pi T}}\exp(-\frac{E_{per}+\frac{1}{2}m(v_{parlab}-v_s)^2}{T}) \quad ,$$

where E_{per} is the transverse energy of the particle for a given parallel velocity v_{parlab}. As for the TLF and PLF sources, we can calculate the average particle transverse energy $<E_{tr}>$ as a function of v_{parlab}. In this case, $<E_{tr}>=T$, independently of v_{parlab}. To take into account relativistic effects and for a proper treatment of the kinematics, we use the relativistic equivalent [26] of these formula (which are cumbersome to write). These relativistic corrections, negligible at 32 A.MeV may amount to ~10% at 95 MeV bombarding energy.

In the fitting procedure, the particle rapidity spectra and their average transverse energy $<E_{tr}>$ as a function of the rapidity are fitted simultaneously. The energy detection thresholds, the detector thickness and the geometry of INDRA are taken into account. In the three-source fit, N_{TLF}, N_{MR}, N_{PLF}, T_{TLF}, T_{MR}, T_{PLF}, Y_{TLF}/Y_P, Y_{MR}/Y_P and Y_{PLF}/Y_P were considered as free parameters. The N's, Ts and Y/Y_P's are the intensities, the temperatures and the reduced rapidities of the sources respectively, Y_P being the rapidity of the projectile. For protons, as we are dealing with light projectile and target, we have neglected the Coulomb barriers in the PLF and in the TLF. The results of the fits for protons at 95 A.MeV bombarding energy are shown in fig. 3. The rapidity spectra as well as the transverse energies are remarkably well reproduced by the fits. The mid-rapidity component peaked at value, Y_{MR}/Y_P, slightly below 0.5 almost covers the whole rapidity range and extends well underneath the TLF and PLF sources. Thus, it is not possible to unfold the different components on an event by event basis. One notes also the strong increase of the mid-rapidity component as the PLF atomic number, Z_{max}, decreases (decreasing impact parameter). For $Y/Y_P<0.2$, the transverse energy increases, indicating that in this region the mid-rapidity contribution decreases less rapidly than the TLF contribution. One expects the same effect on the PLF side above $Y/Y_P>1.2$. However, at 95 A.MeV bombarding energy, at the most forward angles, the proton range is greater than the detector thicknesses, explaining the continuous decrease of the transverse energy for high values of Y/Y_P. For bombarding energies $E_{lab}\leq 74$ A.MeV, the detector thickness is sufficient to stop the protons whatever the emission angle and we observe the increase in the transverse

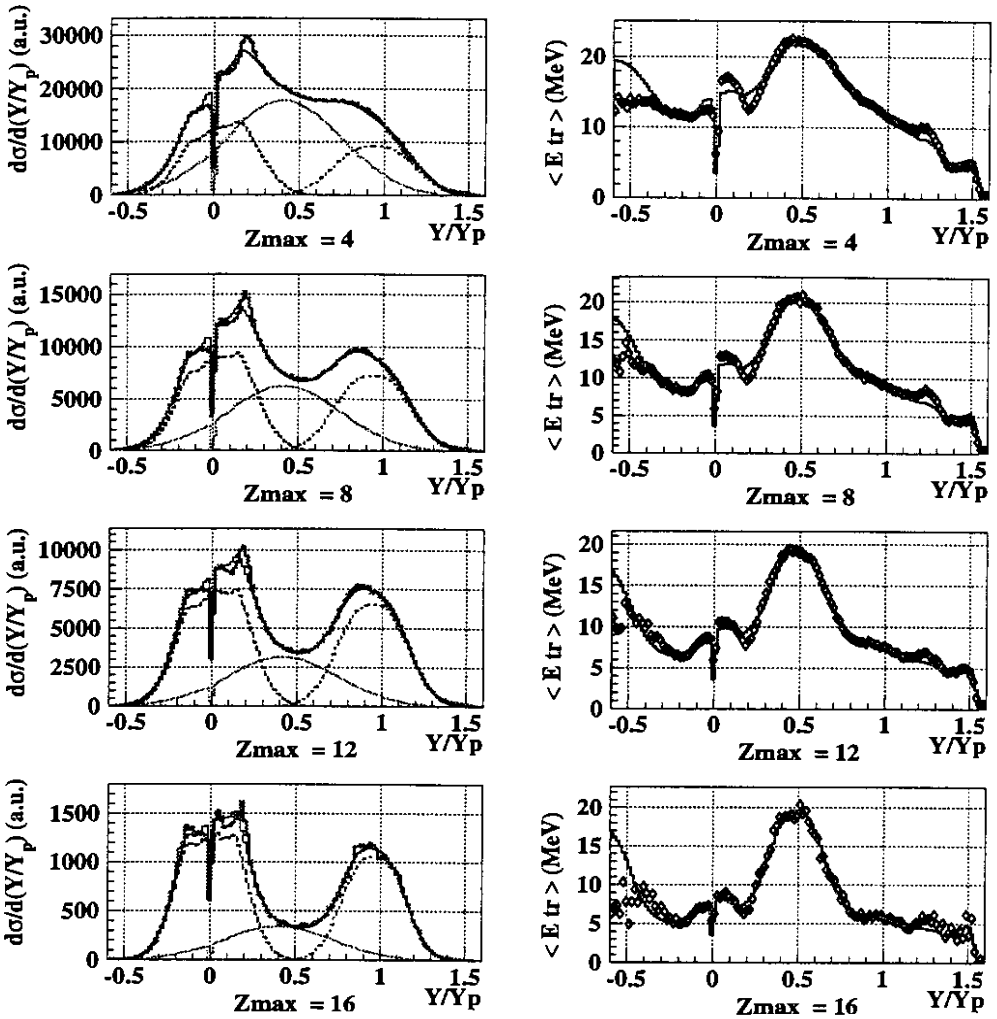

Fig. 3. *Left panel*). Protons rapidity spectra at 95 A.MeV bombarding energy for 4 different values of the PLF atomic number Z_{max}. The data are shown by the full grey curves. The results of the fits are indicated by the full black curves. The TLF, MR and PLF components are shown by the dashed, the dotted and the dash-dotted curves respectively. *Right panel*). Average proton transverse energies, $<E_{tr}>$ as a function of rapidity for the same 4 values of the PLF atomic number Z_{max}. The data are represented by the open diamonds whereas the results of the fits are shown by the full grey curves.

energy for $Y/Y_P>1.2$. The same analysis was performed for all PLF atomic numbers such that $2\leq Z_{max}\leq 16$. and at all bombarding energies from 32 to 95 A.MeV, yielding the same quality of fits. The results obtained at 95 A.MeV are summarized in fig. 4 which displays the evolution of the source parameter as a function of the PLF atomic number Z_{max} (impact parameter). For a given source at a given impact parameter, the reduced contribution is defined as $N_s/(N_{TLF}+N_{MR}+N_{PLF})$ and the multiplicity as N_s/N_{QP}, where the index, s, stands for TLF, MR or PLF and N_{QP} is the number of PLF having the atomic number Z_{max}. The temperatures of the TLF and PLF sources increase slowly with decreasing impact parameter from ~3 MeV for peripheral collisions (Z_{max}=16) to ~5 MeV, for central collisions (Z_{max}=2), the temperature of the PLF source being slightly higher that the TLF one's. By contrast, the temperature of the MR source is very high, increasing from 20 MeV in peripheral collision to 23 MeV in central

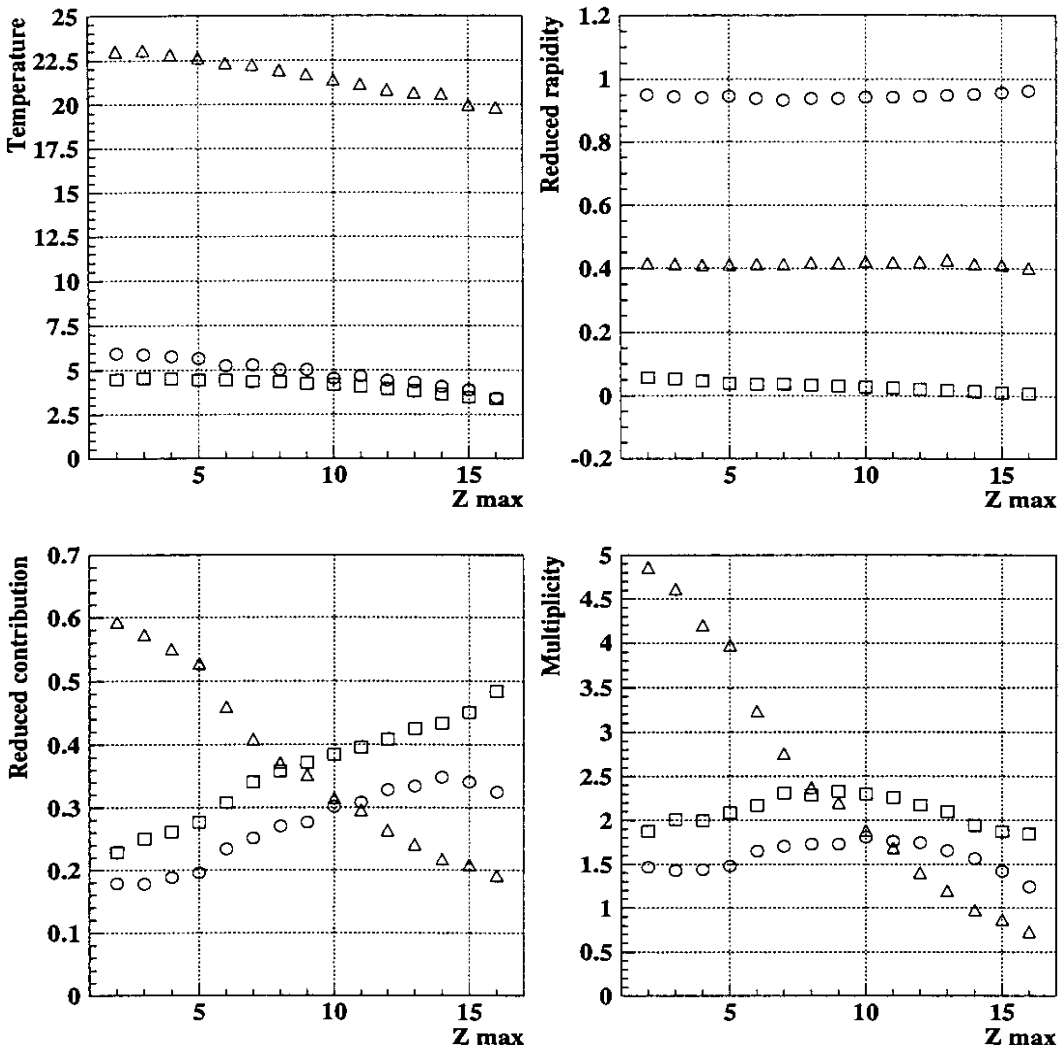

Fig. 4. Evolution of the TLF (□), MR (Δ) and PLF (o) source parameters as a function of the PLF atomic number, Z_{max}, for proton emission in the reaction ^{36}Ar+^{58}Ni at 95 A.MeV bombarding energy.

collisions. We note that these values are close to the available energy per nucleon (22.3 A.MeV) in the center of mass. The PLF source reduced rapidity (Y_{PLF}/Y_P≈0.95) does not evolve much with the impact parameter whereas the reduced rapidity, Y_{TLF}/Y_P, of the TLF source increases from ~0.0 to ~0.05 from peripheral to central collisions. The reduced rapidity Y_{MR}/Y_P of the MR source is approximately constant at ~0.4, a value which is only slightly higher than the reduced rapidity of the center of mass, Y_{cm}/Y_P=0.383. This observation tends to show that the region of overlap between the projectile and the target is at the origin of the mid-rapidity emission. The proton multiplicities from the TLF and PLF sources show the same evolution: they increase from peripheral (Z_{max}=16) collisions to reach a maximum for mid-peripheral (Z_{max}=9) and then decrease towards central collisions (Z_{max}=2). As the temperatures of both sources increase (slightly) with decreasing impact parameter, this behavior can only be understood if we assume that the sizes of the sources decrease with decreasing impact parameters. We note also that the TLF and PLF proton multiplicities are in the target to projectile mass ratio as expected from two nuclei having approximately the same temperature. By contrast, the MR proton multiplicity increases strongly and monotonously from peripheral to central collisions, to become the dominant source of protons in mid-periph-

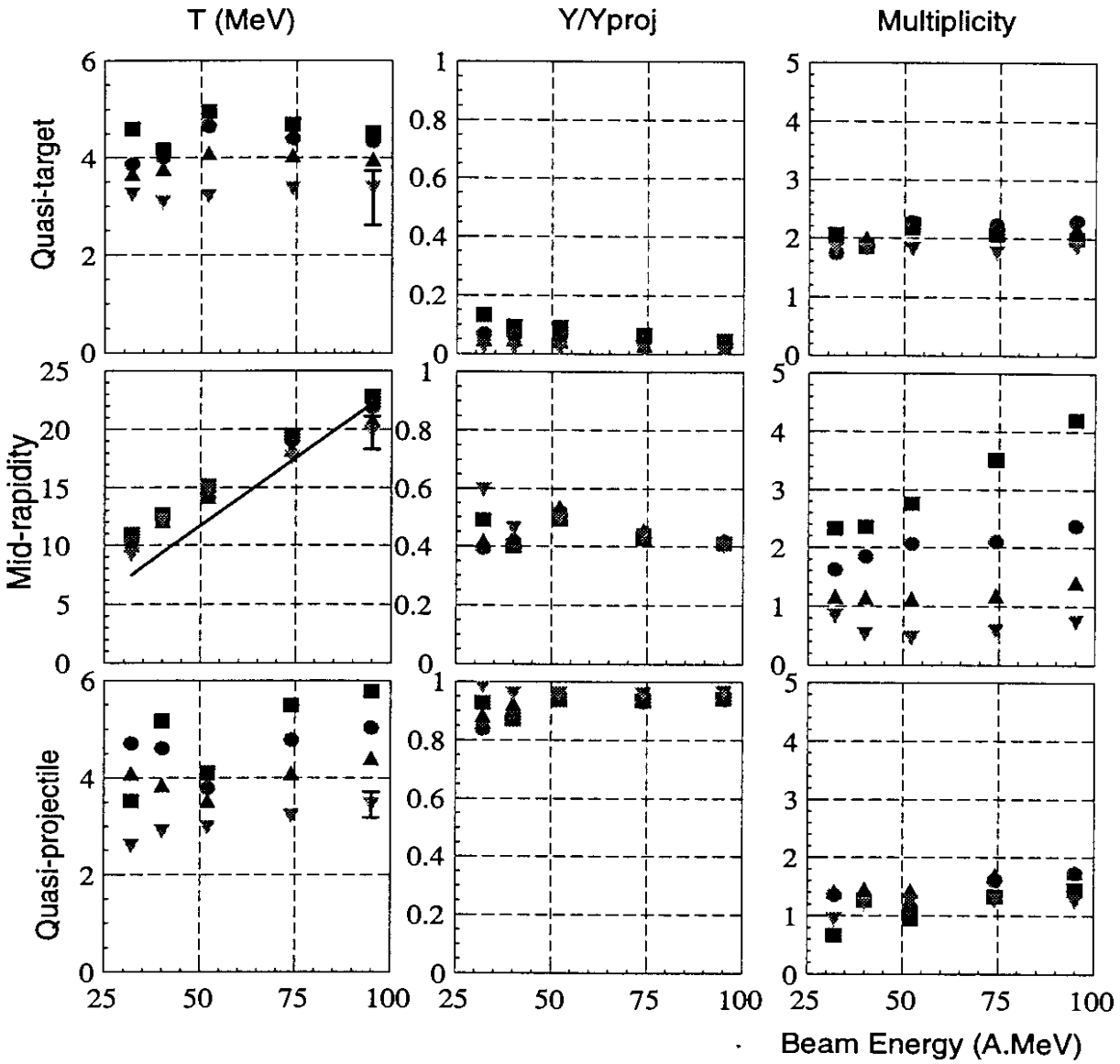

Fig. 5. Evolution with bombarding energy of the source parameters for protons emitted in the $^{36}Ar+^{58}Ni$ reaction for 4 different impact parameters selected by the PLF atomic number, Z_{max}=16 (▼), Z_{max}=12 (▲), Z_{max}=8 (●) et Z_{max}=4 (■). The parameters are given respectively for the PLF (upper row), the MR(center row) and the TLF (lower row) sources.

eral to central collisions. All these observations tend to reinforce the geometric aspect of the collisions.

The evolution with bombarding energy of the source parameters for proton emission are summarized in fig. 5. For a given impact parameter (fixed Z_{max} value), the TLF and PLF temperatures do not evolve much with bombarding energy. On the contrary, the temperature of the MR source increases linearly with bombarding energy and follows closely the available energy in the center of mass indicated by the full line in the figure. As far as the reduced rapidities of the sources are concerned, they do not evolve much with bombarding energies except at the two lowest energies, 32 and 40 A.MeV. The TLF proton multiplicity stays remarkably constant at about 2, whatever the impact parameter or the bombarding energy. The PLF proton multiplicity, almost independent of the impact parameter, increases slightly

with bombarding energy, from about 1 at 32 A.MeV to about 1.5 at 95 A.MeV. There again, the strongest evolution is seen for the MR source. For peripheral to mid-central collisions the proton multiplicity is practically independent of the bombarding energy. For more central collisions (Z_{max}=4), the proton multiplicity increases almost linearly with bombarding energy. As we will see later, this increase corresponds to a decrease in the α-particle production.

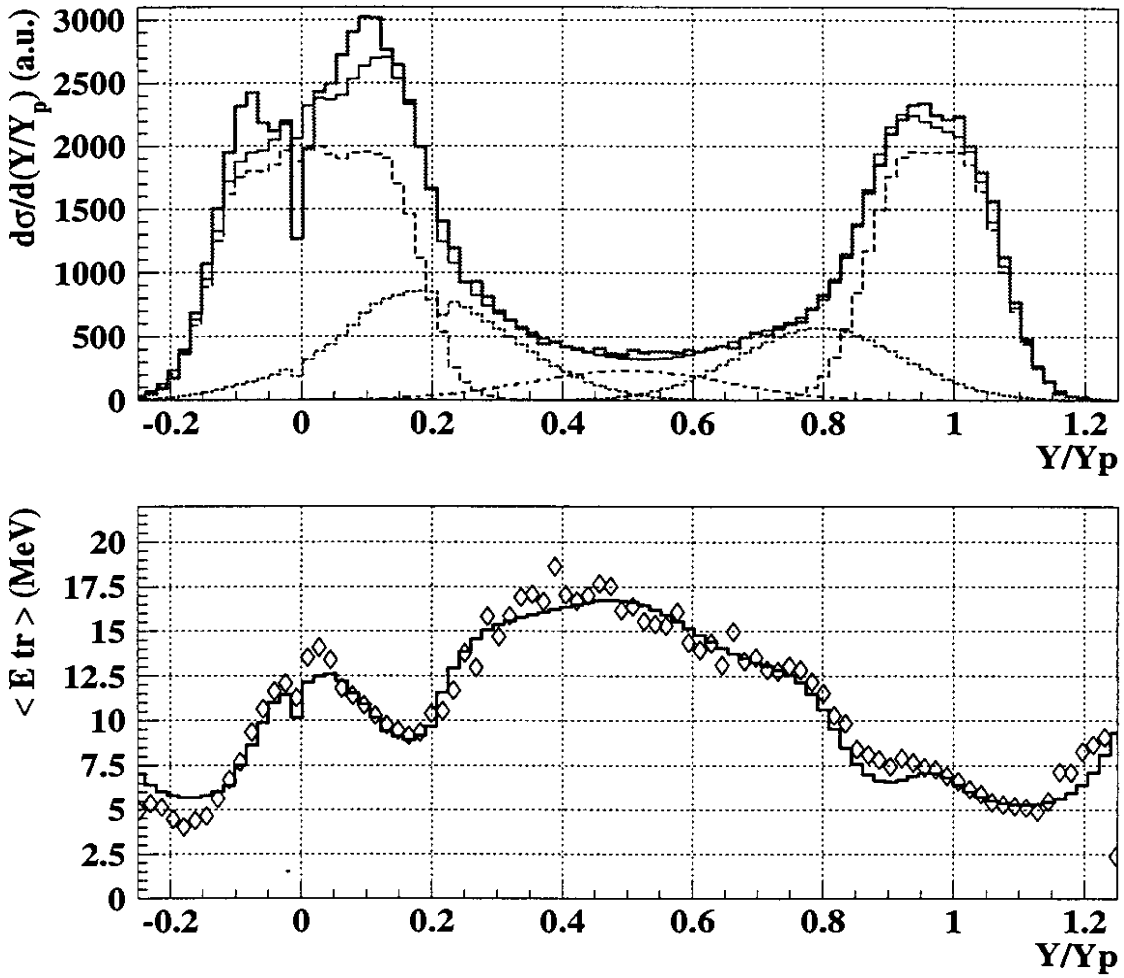

Fig.6. *Top panel*) Experimental rapidity spectrum (grey curve) for α-particles produced in the ^{36}Ar+^{58}Ni at 95 A.MeV bombarding energy for peripheral collisions in coincidence with a PLF of Z_{max}=14. The overall fit is indicated by the dark curve. The TLF and PLF components are shown by the dashed curves, the MR component, by the dot-dashed curve and the two sources corresponding to nucleon-α and α-nucleon scattering by the dotted curves. *Bottom panel*) Average transverse energy $<E_{tr}>$ as a function of the reduced rapidity for the same α-particles. The data are the open diamonds, the result of the fit is given by the black curve.

Using the same formalism, taking into account the PLF and TLF Coulomb barrier as given by the systematic [27, 28], we have attempted to fit the rapidity spectra of α-particles and their average transverse energy, $<E_{tr}>$ as a function of rapidity, neither could be reproduced satisfactorily. The origin of this difficulty was found in the fact that in the experimental α-particles rapidity spectra, in the front of the TLF source at Y/Y_P~0.2 and in the back of the

PLF source at Y/Y_P~0.8, there is always an excess of high energy α-particles which cannot be explained by a simple evaporation from the TLF or the PLF as it has been observed previously [11]. The values of Y/Y_P, 0.2 and 0.8 correspond closely to the nucleon-α and α-nucleon reduced rapidities respectively. Thus some of the observed α-particles may originate from a collision between a nucleon of the projectile and an α-cluster in the target and vice-versa. To simulate this type of emission, two identical volume emitting sources where added at the nucleon-α and α-nucleon rapidities respectively. The resulting fits are shown on fig.6 for α-particles emitted in coincidence with a PLF of Z_{max}=14 (peripheral collisions) at 95 MeV bombarding energy. The agreement with the experimental data is excellent. The same type of agreement is obtained for all impact parameters ($2 \leq Z_{max} \leq 16$) and all bombarding energies from 50 to 95 A.MeV. However, it was not possible to give a proper description of the data at 32 and 40 A.MeV bombarding energies. At these energies, the MR component is much less apparent and it seems that there is a change in the reaction mechanism as evidenced from other observables. Hence, the PLF atomic mass distributions [29] evolve from 32 to 50 A.MeV to remain identical up to 95 A.MeV bombarding energy. As far as the TLF, PLF and MR sources are concerned, from 50 to 95 A.MeV bombarding energies, their parameters (temperature and reduced rapidity), follow quite closely the evolution given for the protons in figs. 4-5 and are practically indistinguishable. For the nucleon-α and α-nucleon sources, their temperature is about 70% of the temperature of the MR component and follow the same evolution with impact parameter and bombarding energy. For a fixed impact parameter (a given Z_{max}), contrary to what is observed for the protons, the α-particle multiplicity decreases slightly with bombarding energy. This decrease is completely compensated by an increase of the proton multiplicity in such a way that the quantity of emitted charge remains constant. As we bring more and more energy in the region of overlap between projectile and target, it becomes possible to destroy more and more clusters.

4. Summary and conclusions

The rapidity spectra and the average transverse energies as a function of rapidity of protons and α-particles produced in the $^{36}Ar+^{58}Ni$ reaction have been analyzed as a function of the impact parameter and the bombarding energy from 32 to 95 A.MeV. The proton data are quite well reproduced assuming three sources of emission, excited TLF's and PLF's and a third MR source localized at a rapidity close to the center of mass rapidity. For the α-particles, there is in the data an excess of particles with high transverse energies emitted forward of the TLF and backward of the PLF which cannot be easily explained by evaporation from fully equilibrated PLF's and TLF's. A possible explanation is given by nucleon-α and α-nucleon collisions in the region of overlap between projectile and target. Furthermore, there seems to be a transition in the reaction mechanism around 50 A.MeV bombarding energy. The number of particles emitted around mid-rapidity increases almost

linearly with decreasing impact parameter. The proton and α-particle transverse energies, close to the center of mass rapidity, are the same and almost independent of the impact parameter. They increase linearly with the bombarding energy with values close the available energy in the center of mass. Above 50 A.MeV, for a given PLF atomic number, the quantity of charged produced around mid-rapidity become independent of bombarding energy. The slight decrease in α production is compensated by an increase in the proton production. This observation has to be correlated with the fact that the PLF atomic charge distributions become independent of bombarding energy above 50 A.MeV. Both effects may be explained by geometrical considerations: as the impact parameter decreases the region of overlap between

projectile and target increases. Most of the energy is dissipated in this overlap region giving rise to the mid-rapidity emission whereas the remaining of the projectile and the target are moderately excited to a level which becomes independent of the incident energy.

From the present analysis, it is found that the particles produced in the overlap region cover the whole rapidity range and extend over the TLF and PLF evaporating region rendering the separation between the different sources almost impossible on an event by event basis. The TLF and PLF source temperatures are relatively low compared to a previous analysis [30] in which the PLF temperatures were determined from the particles emitted in the forward hemisphere only in order to eliminate some possible contamination from the mid-rapidity zone. It should be noted that in this case, the extracted temperatures are very sensitive to the velocity assumed for the source. In the present analysis, the TLF and PLF temperatures increase from about 2.5 MeV in peripheral to about 5 MeV in central collisions. Above 50 MeV bombarding energy and for a given impact parameter these temperatures become independent of the incident energy in agreement with the geometrical hypothesis.

It would be interesting to pursue the same analysis for other charged particles in order to determine the quantity of matter evaporated by the PLF's and TLF's. Thus it would be possible to determine the size and the excitation energy of the primary fragments as a function of the impact parameter and the beam energy as it has been attempted in [24] for the same reaction at 95 A.MeV bombarding energy

References.

[1] D. Guerreau, Nucl. Phys. **A447** (1986) 37c.

[2] R. Dayras, J.Phys. (Paris), Colloq. 47 (1986) C4-13.

[3] B. Borderie, M.F. Rivet and L. Tassan-Got, Ann. Phys. Fr. **15** (1990) 287.

[4] H. Fuchs and K. Möhring, Rep. On Prog. in Phys. **57** (1994) 231.

[5] R. Dayras *et al.*, Nucl. Phys. **A460** (1986) 299.

[6] D.J. Morrissey, L.F. Oliveira, J.O. Rasmussen, G.T. Seaborg, Y. Yariv and Z. Fraenkel, Phys. Rev. Lett. **43** (1979) 1139.

[7] R. Dayras *et al.*, Phys. Rev. Lett. **62** (1989) 1017.

[8] T.J.M. Symons *et al.*, Phys. Lett. **94B** (1980) 131.

[9] J.C. Steckmeyer *et al.*, Nucl. Phys. **A500** (1989) 372.

[10] L. Stuggé *et al.* Nucl. Phys. **A539** (1992) 511.

[11] J.E. Sauvestre *et al.*, Phys. Lett. **B335** (1994) 300.

[12] J. Péter *et al.*, Nucl. Phys. **A593** (1995) 95.

[13] J. Pouthas *et al.*, INDRA coll., Nucl. Inst. and Meth. **A357** (1995) 418.

[14] V. Métivier *et al.*, INDRA coll., Nucl. Phys. **A**., *in press*

[15] J. Lukasik *et al.*, INDRA coll., Phys. Rev. **C55** (1997) 1906.

[16] E. Plagnol *et al.*, INDRA coll., Phys. Rev. **C61** (1999) 014606.

[17] A. Stefanini *et al.* Z. Phys. **A351** (1995)167.

[18] F. Bocage *et al.*, INDRA and Nautilus coll., submitted to Nucl. Phys. A

[19] T. Lefort *et al.*, INDRA coll., Nucl. Phys. **A662** (2000) 397.

[20] P. Sapienza et al., Nucl. Phys. **A630** (1998) 215c and these Proceedings

[21] F. Haddad, Ph. Eudes, Z. Basrak and F. Sébille, Phys. Rev. **C60** (1999) 031603.

[22] P. Pawlowski *et al.*, INDRA coll., to be published.

[23] D. Doré *et al.*, INDRA coll., in preparation.

[24] D. Doré *et al.*, INDRA coll., to be published.

[25] C. Cavata, M. Demoulins, J. Gosset, M.-C. Lemaire, D. L'Hôte, J. Poitou and O. Valette, Phys. Rev. **C42** (1990) 1760.

[26] T.C. Awes, G. Poggi, S. Saini, C.K. Gelbke, R. Legrain and G.D. Westfall, Phys. Lett. **B103** (1981) 417.

[27] J.M. Alexander, D. Guerreau et L.C. Vaz, Zeit. Phys. **A305** (1982) 313.

[28] M.F. Rivet, D. Logan, J.M. Alexander, D. Guerreau, E. Duek, M.S. Zisman and M. Kaplan, Phys. Rev. **C25** (1982) 2430.

[29] Ph. Buchet, PhD thesis, Caen 1999.

[30] Y.G. Ma *et al.*, INDRA coll., Phys. Lett. **B390** (1997) 41.